

Sensitive quantification and morphological analysis of microfibers in laundry wastewater:
Standardization and validation of a fluorescence-based method

Original

Sensitive quantification and morphological analysis of microfibers in laundry wastewater: Standardization and validation of a fluorescence-based method / Lupato, S., Granetto, M., Tiraferri, A., Sethi, R.. - In: JOURNAL OF HAZARDOUS MATERIALS. - ISSN 0304-3894. - 495:(2025). [10.1016/j.jhazmat.2025.138947]

Availability:

This version is available at: 11583/3001441 since: 2025-07-01T17:36:16Z

Publisher:

Elsevier B.V.

Published

DOI:10.1016/j.jhazmat.2025.138947

Terms of use:

This article is made available under terms and conditions as specified in the corresponding bibliographic description in the repository

Publisher copyright

(Article begins on next page)



Sensitive quantification and morphological analysis of microfibers in laundry wastewater: Standardization and validation of a fluorescence-based method

Silvia Lupato ^a , Monica Granetto ^a, Alberto Tiraferri ^{a,b,*}, Rajandrea Sethi ^{a,b,*}

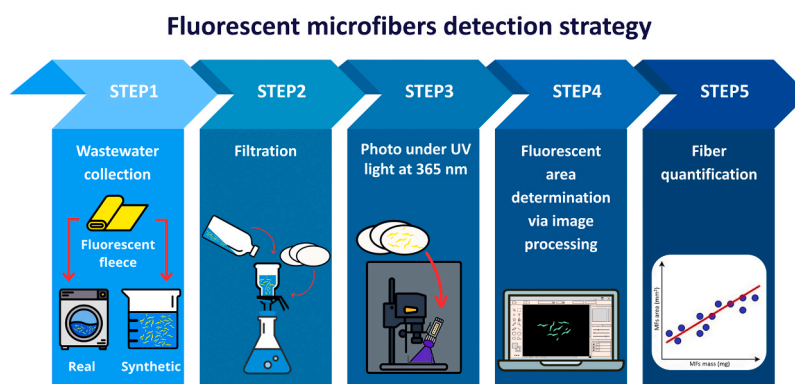
^a Department of Environment, Land and Infrastructure Engineering, Politecnico di Torino, Corso Duca degli Abruzzi 24, Torino 10129, Italy

^b Clean Water Center (CWC), Politecnico di Torino, Corso Duca degli Abruzzi 24, Turin 10129, Italy

HIGHLIGHTS

- High accuracy standardized method detects fluorescent microfibers in wastewater.
- Method achieves microfibers quantification with a detection limit of just 1 µg.
- Automated image analysis for rapid, low-cost microfiber counting and measurement.
- Microfiber fragmentation during laundering leads to shorter fibers in wastewater.
- Washing machine wastewater samples had an average microfiber length of 1.13 mm.

GRAPHICAL ABSTRACT



ARTICLE INFO

Keywords:

Microfibers (MFs)
Microplastics
Fluorescence
Laundry wastewater
Morphological analysis

ABSTRACT

Microplastics and microfibers are widespread environmental pollutants, with synthetic microfibers comprising 40–90 % of microplastics in aquatic systems. Accurate quantification is essential for assessing and mitigating their impact, but conventional methods face several challenges, including high costs, labor-intensive procedures, and limited accessibility. This study standardizes and validates a cost- and time-effective fluorescence-based method for the sensitive detection and automated quantification of polyester-based microfibers. Exploiting the fluorescence properties of polyester fibers under UV light, the method enables direct visualization and automated quantification of the fibers from images obtained using a simple camera setup through open-source software. The method was developed using synthetic, fluorescent microfiber suspensions with concentrations ranging from 1 µg/L to 125 µg/L and processed through glass-fiber filters. This procedure yielded a linear calibration curve ($R^2 = 0.987$) between the automatically computed fluorescent area on the filter surface and the mass of filtered microfibers weighted on an analytical balance. The limit of detection (LOD) and quantification (LOQ) were estimated to be 1 µg and 2.5 µg, respectively, demonstrating high sensitivity. Validation with washing machine wastewater samples showed excellent accuracy, with computed concentrations through fluorescence aligning

* Corresponding authors at: Department of Environment, Land and Infrastructure Engineering, Politecnico di Torino, Corso Duca degli Abruzzi 24, Torino 10129, Italy.

E-mail addresses: alberto.tiraferri@polito.it (A. Tiraferri), rajandrea.sethi@polito.it (R. Sethi).

<https://doi.org/10.1016/j.jhazmat.2025.138947>

Received 10 March 2025; Received in revised form 22 May 2025; Accepted 14 June 2025

Available online 16 June 2025

0304-3894/© 2025 The Authors. Published by Elsevier B.V. This is an open access article under the CC BY-NC-ND license (<http://creativecommons.org/licenses/by-nc-nd/4.0/>).

closely with known suspension values. Additionally, the method quantified total fiber length and number, showing a strong correlation between fiber length and area. Morphological analysis revealed shorter fiber lengths in wash water samples compared to synthetic fibers with an average of 1.13 mm and 2.31 mm, respectively, likely due to fragmentation during laundering. Furthermore, washing machine wastewater samples consistently had higher fiber counts, indicating increased fragmentation. These findings highlight the method's robustness, adaptability, and potential for broad applications, allowing for both quantitative and morphological microfiber analysis in environmental and industrial settings, while also contributing to the development of future reference standards.

1. Introduction

Microplastics (MPs) - plastic fragments with average dimensions below 5 mm [1] - have become a widespread contaminant [2,3] and a major environmental concern [4–6]. These pollutants are widely dispersed due to the biological, chemical, and physical degradation of plastic products [7,8] during their end-of-life phase, along with the extensive use of synthetic polymers across various industrial sectors [9]. Their prevalence now affects all environmental compartments, with aquatic systems being particularly impacted [10]. Among the primary contributors to MPs pollution in water are synthetic microfibers (MFs) [11], accounting for 40–90 % of the MPs in water and sediments [12]. MFs are defined as the subcategory of MPs generically characterized by diameters below 10 μm [13] or, more specifically, as fibers with a length between 1 μm and 5 mm, characterized by a length to diameter ratio over 100 [12]. The extensive use of synthetic textiles makes domestic laundry wastewater a major source of MFs [14], with global estimates indicating that household laundering contributes up to 35 % of MP emissions into the environment [15]. With stricter regulations being implemented and new limits on MP and MF emissions expected in the coming years [16], there is an urgent need for cost-effective and standardized methods to detect and quantify these pollutants, enabling

effective monitoring, planning of mitigation measures, and reduction of environmental and health impacts [17].

Given the diverse sources and environmental processes affecting MFs [18,19], their morphological characteristics may vary widely [20,21]. However, efforts to establish standardized analytical methodologies have largely converged on some commonly employed techniques [22–26]. Table 1 summarizes the principal characteristics of the most employed techniques for MFs analysis in water samples, each characterized by distinct advantages and limitations [24,26]. Scanning electron microscopy (SEM) is widely employed for high-resolution morphological characterization of fibers and fabrics, offering detailed imaging capabilities that are essential for studying the physical structure of MFs [27]. However, SEM requires conductive samples and meticulous preparation, which can introduce inaccuracies if not properly managed. Fourier-transform infrared spectroscopy (FT-IR) and Raman spectroscopy are among the most used methods for chemical characterization. These techniques enable precise polymer identification, making them particularly useful for analyzing MFs in complex samples, such as laundering wastewater [28,29]. Despite their utility, they are susceptible to interference from external contaminants, and may be limited by fluorescence interactions [30]. Their microscopic variants, micro-FTIR and micro-Raman, integrate imaging and particle quantification [31],

Table 1

Assessment of the main analytical techniques applied to MF detection, characterization, and quantification [23,24,26].

Technique	Strengths and limitations	Objective	Sample size, scale of the analysis, and typically required time.	References
SEM	High-resolution imaging; visualizes morphology, structure, and length of MFs; quantifies MFs through counting. Requires conductive samples; labor-intensive preparation; may alter/damage samples; requires skilled operator; requires several images for statistical representativeness.	Visual and morphological analysis; quantification.	Sample size: > 2 mm if solid; > 100 μL if liquid. Image size: $\sim 1\text{--}10 \mu\text{m}^2$ per image. min to hours for sample preparation and imaging.	[27,40–42]
FT-IR	Rapid data acquisition; minimal sample material required; non-destructive; suitable for polymer identification. Qualitative; sensitive to environmental factors (e.g., water/solvents); analyzed portion may not be representative of the entire sample.	Polymer identification.	Sample size: > 15–25 μm depth for pure liquids; 0.1–1.0 mm depth for suspensions; few mm with particles > 10 μm for solids. s to minutes for sample preparation and measurement.	[28–30,43,44]
Raman	Non-destructive; works with various sample states (solid; liquid; gaseous); can differentiate similar polymers. Qualitative; susceptible to fluorescence interference; analyzed portion may not be representative of the entire sample.	Polymer identification.	Sample quantity: ~ 1 g for solids, ~ 20 mL for liquids; particle size of few mm. Detection size: $\sim 1 \mu\text{m}$ for solids. min to hours for sample preparation and analysis.	[28,30,45]
μ -FTIR and μ -Raman	Combines advantages and disadvantages of conventional Raman, FTIR, and microscopy techniques, while providing a more comprehensive result in one single analysis.	Polymer identification; quantification; visual and morphological analysis.	Sample size: 5–10 μm depth for aqueous/gel samples with μ -FTIR; 5–20 μm in depth for aqueous/gel samples with μ -Raman. A few minutes to seconds for sample preparation. Analysis time directly proportional to the sample size (may take hours)	[31,46,47]
MS/GC	Detailed molecular analysis; identifies polymer and chemical composition; semi-quantitative. Destructive; labor-intensive; requires specialized expertise and instrumentation; high operational cost; less effective for non-volatile compounds	Molecular structure; chemical composition.	Sample quantity: 5–200 μg without pretreatment. h for sample preparation and analysis.	[33,34,48,49]
TOC	Quantitative; low to medium detection limits; reliable for carbon-based materials. Time-consuming for solid samples; requires several replicates for robustness; technical issues may arise with liquid samples that are not well-dispersed.	Quantitative carbon analysis.	Sample quantity: sub- μg to sub-mg amounts for solids; 25–100 mL per sample for liquid samples. Detection limit: $\sim 7 \mu\text{g/L}$. $\sim 15\text{--}20$ min per sample (sample preparation and analysis)	[34,35,50]

as well as polymeric structure characterization [32]. While they offer the advantage of obtaining multiple results from a single analysis, they are time-consuming and inherit the limitations of their standard counterparts. Gas chromatography-mass spectrometry (GC-MS) provides another robust option for chemical analysis. By examining decomposition products, GC-MS offers insights into the molecular composition of MFs, complementing spectroscopic methods [33]. However, GC-MS requires extensive sample preparation and technical expertise, limiting its suitability for routine analyses [34]. Total organic carbon (TOC) analysis provides high sensitivity in quantifying MF concentrations down to 0.1 mg/L, but may be affected by the presence of organic matter, leading to potential overestimations or inaccuracies, particularly in samples with low MF content [34,35]. Nile Red staining enhances MP and MF detectability under UV light for improved analysis. However, different polymers exhibit varying responses to uniform staining and fluorescence conditions, requiring substantial improvements for accurate detection and quantification [36–39]. This overview of techniques implies that no single method yields comprehensive results on its own, making the integration of multiple approaches essential for effective microfiber analysis. Advancing current methodologies and developing standard techniques are crucial for improving detection and quantification accuracy, enhancing reliability, and minimizing costs.

Recent studies have explored approaches combining different and novel techniques for improved MF identification and quantification. For example, Tian *et al.* [51] proposed a methodology coupling MS and FT-IR and relying on empirical equations rather than direct MF quantification. Similarly, Lim *et al.* [52] combined MS and FT-IR analyses with selective solvent extraction for better MF separation and quantification. Galvão *et al.* [53] quantified MF release from simulated household washing cycles through microscopy and direct fiber counting, using known material composition and aging effect as a standard to distinguish fibers by morphology and color. Haap *et al.* [54] suggested an analytical approach based on a chemical separation process to differentiate cotton and synthetic fibers, followed by dynamic image analysis. Serranti *et al.* suggested MP and MF identification through hyperspectral imaging, defining different setups depending on the particle size [55], whose efficiency was later proven through analyses on water samples [56]. Differently, Napper *et al.* [57] proposed a method focused solely on quantifying microfibers by number, based on an empirical relationship with the known initial mass of microfibers, with fiber imaging performed using optical light microscopy. This method was also adopted by De Falco *et al.* in their recent studies on synthetic microfibers [58, 59].

All these techniques face significant challenges. High costs, complex operation, and the need for specialized training often limit accessibility, particularly in resource-constrained settings. Their labor-intensive workflows further hinder their applicability for large-scale or rapid assessments, and the lack of a unified analytical approach frequently necessitates combining multiple methods, increasing complexity and cost. Additionally, inconsistent reporting units (e.g., MF count vs. MF mass per volume) diminishes results comparability [21], further complicating comprehensive MF characterization. These limitations highlight the urgent need for innovative methodologies that balance accuracy, scalability, affordability, and efficiency for effective MF monitoring and mitigation [60]. Recently, an improved fluorescent-based method was introduced, applying different excitation wavelengths and fluorescent filters to better differentiate PET and other polymers with fluorescent microscopy [61]. Another study assessed the feasibility of better identifying plastic polymers under UV light sources [62]. This method holds promise for the rapid and automated analysis of environmental samples, but the authors highlighted the need for standardization and further improvement aiming at more easily scalable approaches [61,63]. Recently, fluorescence-based techniques for the identification and characterization of microfibers and microplastics have also been explored. For instance, two studies proposed the use of laser-induced fluorescence (LIF) combined with principal component analysis (PCA) and microscopy, leveraging the intrinsic fluorescence properties of plastics to improve detection and classification [64,65]. In contrast, other approaches rely on fluorescent dyes to label microplastics and microfibers, facilitating their identification through fluorescence-based detection methods [66,67].

This study seeks to build upon recent research with the goal of standardizing and validating a cost- and time-effective, technique for detecting and quantifying fluorescent MFs. Notably, the methodology is based on the use of a simple setup consisting of a photographic camera and a UV lamp, combined with programmed image processing. The standardized method involves filtering the MF suspension, visualizing the filter under UV light, and quantifying the fluorescent area using software for an automated analysis of the collected pictures. Therefore, this method offers a cost- and time-efficient alternative to conventional techniques based on microfiber imaging, by capturing all fluorescent microfibers filtered from a suspension in a single image without the need of post-processing steps, e.g., photo stitching. Specifically, this manuscript presents the method details and its calibration using synthetic suspensions of polyester microfibers with known mass concentrations, used to establish its accuracy and reliability. The method's validation

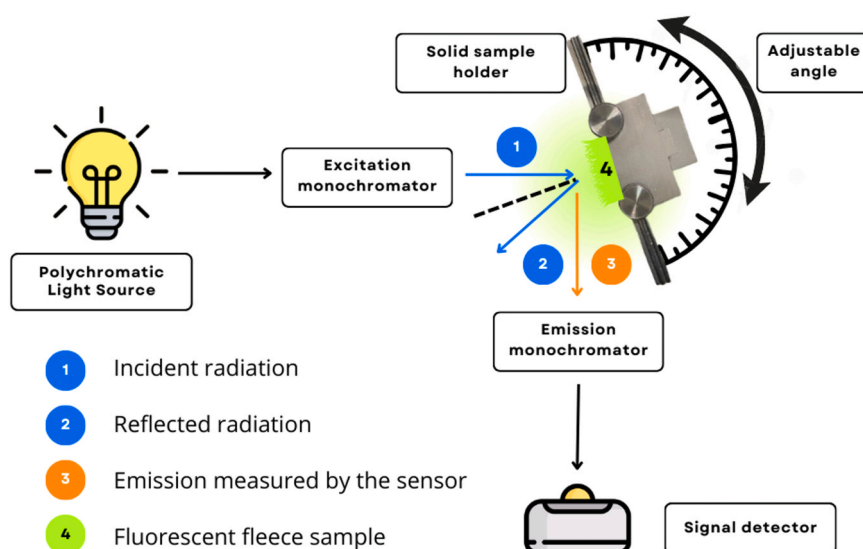


Fig. 1. Spectrofluorometer functioning scheme in front face mode, used for the characterization of all the solid materials.

and application are then discussed, utilizing laundry wastewater containing microfibers released from a polyester garment. Additionally, the study examines microfiber numbers and morphology, focusing on fiber length distribution.

2. Materials and methods

The methodology standardized in this study comprises three key steps: (i) preparation of microfiber suspensions, (ii) filtration to retain MFs and obtain solid-phase samples, and (iii) MF quantification on filter surfaces using a photographic setup and automated image processing. For its cross-validation, MF quantification was also performed using conventional methods, including direct weighing and total organic carbon (TOC) analysis. The selected materials and detailed protocols for each step are outlined below.

2.1. Materials

A fleece material made entirely of polyester fabric (CRS Fur Fabrics, United Kingdom) was chosen for its fluorescent properties. Comparative materials included cotton fabric and non-fluorescent fleece (Purchased from Ikea, respectively models DVALA and THORGUN). Also, several filters of different materials were tested, including fiberglass filters (Whatman GF/F, diameter of 47 mm and a mesh size of 1.2 μm), cellulose filters (Sartorius, cellulose acetate grade 111), PCB filters (Merck MF Millipore, grade 400), and Teflon filters (Sartorius, grade 118), all of them with a diameter of 47 mm. Deionized water used to prepare suspensions, solutions, and for suspensions and rinsing operations was produced using a Milli-Q system, composed of a Milli-Q E-POD dispenser and a Milli-Q IX-7500 purifying tank (Merck KgaA, Darmstadt, Germany).

2.2. Methods

2.2.1. Materials characterization and filter selection

To determine the optimal wavelength for imaging and configure the photographic setup, the fleece was initially characterized using a Cary Eclipse spectrofluorometer (Agilent - Santa Clara, CA, US). The instrument parameters were set with an excitation slit width of 5 nm and an emission slit width of 2.5 nm. The excitation-emission matrices (FF-EEM) were collected through sample excitation across a wavelength range of 200–800 nm, and emission measurement within the same wavelength range. Measurements were performed in front-face mode using a goniometer-equipped sample holder (Fig. 1). This configuration is more suitable for solid and turbid liquid samples than conventional right-angle configuration [68]. While the results from liquid suspensions

did not allow for a quantitative assessment of the concentration of suspended microfibers in water, the measurements on a piece of textile sample provided valuable insights into its fluorescence properties. Selectivity was assessed by comparing the fluorescence response of the polyester fleece to that of cotton and non-fluorescent fleece. The EEMs of cotton and normal fleece reported in the supporting information (SI), Figure S1, indicate negligible response for these two samples, especially at the desired wavelength of 365 nm, with minimal signal imputable to scattering phenomena. Fiberglass, cellulose, PCB, and Teflon filters were tested under UV illumination to identify a non-fluorescent filter material capable of producing a completely dark background, thereby enhancing the visibility of fluorescent fibers. A clear response was observed in the blue range for cellulose, Teflon, and PCB filters when their photograph was taken under UV light; see Figure S2 of the SI. On the other hand, no response was observed with the glass fiber, which was thus selected as the filtration support due to their transparency under UV light, ensuring instead a clear visualization of fluorescent fibers. Based on these findings and preliminary experimentation, the photographic setup consisted of a commercial camera (Sony Europe B.V., United Kingdom, typically with a spectral sensitivity in the 400–700 nm range), equipped with a long-pass UV filter on the lens, and a UV lamp centered at 365 nm.

2.2.2. Preparation of the microfiber suspensions

To standardize and validate the method, aqueous suspension referred to as “synthetic” suspensions with known concentrations of MFs originated from the fluorescent fleece were initially prepared. MFs were obtained by mechanical abrasion of a new piece of fleece and manually dispersing the fibers into deionized water. Fluorescence-based quantification was developed by preparing a stock solution via gravimetric measurement using a precision analytical balance with a sensitivity of 0.001 mg (Mettler Toledo – Columbus US). Specifically, a precise amount of 4 mg of MFs was weighed and dispersed in 4 L of deionized water, drawing up a nominal stock concentration of 1 mg/L. Test suspensions were then prepared by diluting the stock solution to a final volume of 1 L, with concentrations ranging from 1 mg/L to 0.001 mg/L. Before filtration, all suspensions were stored in glass bottles with HDPE caps to prevent MFs loss and external contaminations. This combination of gravimetric preparation and dilution ensured both accuracy and repeatability across the investigated range. Note that controlled dilutions were performed during the method’s calibration and development phases of this study, to prepare suspensions with known microfiber quantities. In the application of the method, dilution would not be required for typical samples. It would only be recommended in cases where the initial microfiber concentration is particularly high, in order to avoid signal saturation and to facilitate more accurate image processing

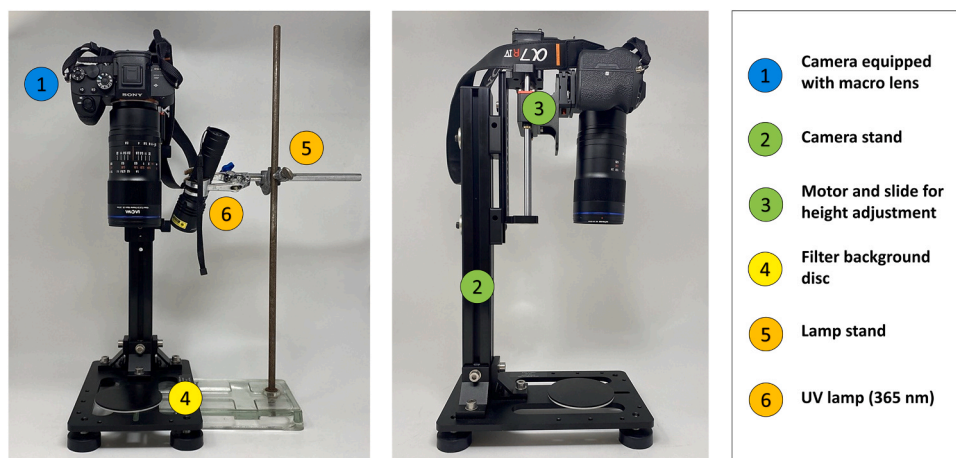


Fig. 2. Photographic setup, front (left) and side (right).

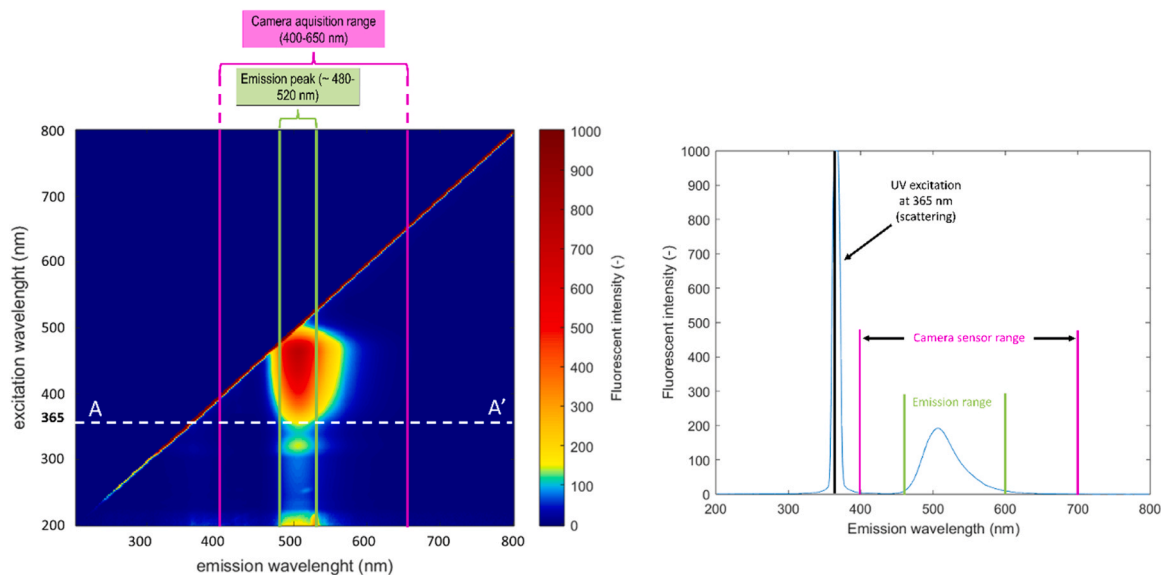


Fig. 3. Fluorescence EEMs of the tested fluorescent fleece (left), and emission peaks at 365 nm of excitation (right).

After validating the method with synthetic suspensions, it was applied to samples obtained from a washing machine (Haier HW80, Germany). For these tests, laundry cycles were performed with a single fluorescent polyester fleece piece measuring 90×80 cm placed in the machine drum. To minimize cross-contamination, a 15-minute blank washing cycle without any fabric was run before each test. The operating conditions for the laundry cycles were standardized as follows: washing time of 77 min, temperature set to 40°C , rotational speed of 1400 rpm. During each cycle, the washing machine discharged wastewater four times, producing a total average volume of 50 L per cycle. The final stock suspension for analysis was prepared by homogenizing the wastewater and extracting a representative aliquot from each discharge, resulting in a combined volume of 1 L. This stock was then diluted with deionized water using appropriate dilution factors before proceeding with subsequent steps of the methodology. Similarly to synthetic suspensions, MFs concentrations from washing machine samples were validated via gravimetric analysis of the total filtered MFs that were discharged over three washing cycles, yielding average release values.

2.2.3. Preparation of the filters

The vacuum filtration setup for the processing of the suspensions consisted of a vacuum pump/line to generate the required pressure difference for filtration, a sintered glass Buchner funnel consisting of a porous septum with diameter of 50 mm, a top glass with a volume equal to 300 mL and a clamp to securely fasten the two components to prevent leakage. A glass fiber filter (Whatman GF/F filters) with a diameter of 47 mm and a mesh size of $1.2\ \mu\text{m}$, specifically chosen to retain virtually all the MFs was chosen. Each glass fiber filter was only used once. Prior to filtration, the 1-L suspensions were thoroughly mixed to achieve uniform distribution of MFs in water, preventing settling and minimizing fiber loss. To avoid contamination or material loss after filtration, the filters were stored in Petri dishes prior to the MF quantification.

2.2.4. Filter image acquisition and processing

The photographic setup for capturing the filter surface (Fig. 2) was housed in a darkroom to ensure controlled imaging conditions and consisted of several cost-effective components. A Sony $\alpha 7$ camera, equipped with a Laowa 100 mm $f/2.8$ macro lens and a long pass UV filter (395 nm cutoff), was used for high-resolution imaging. A UV lamp emitting at a central wavelength of 365 nm provided excitation, while a motorized camera stand allowed precise height adjustments. A personal

computer with Helicon Remote software facilitated remote camera control and automated image acquisition. Each filter was carefully removed from the Petri dish and placed under the camera, where it was photographed under both visible and UV light using standardized ISO 250, exposure of 0.7, and acquisition time of 1.3 s. Focus and camera-to-filter distance were adjusted in the very beginning of the study and consistently maintained throughout. Both the camera settings and position were kept consistent throughout the study to ensure optimal acquisition of microfiber images and to guarantee repeatable and reproducible results. To enhance contrast, a black opaque disc served as a background, and the UV lamp was positioned at an indirect angle relative to the filter to avoid scattering and excessive fluorescence response. Thereby, the lamp's position and height were kept constant throughout all the analyses.

To quantify the MFs present on the filters, ImageJ software (National Institutes of Health and the Laboratory for Optical and Computational Instrumentation LOCI, University of Wisconsin) was used to automatically determine their projected area. Since the resolution and acquisition conditions of the photographs remained consistent, the software analysis parameters were also standardized throughout the study. These parameters were manually optimized across preliminary trials to enhance fiber identification and ensure accurate area estimation. Specifically, image analysis parameters were calibrated via preliminary experimentation in which fiber diameters measured in ImageJ regions of interest were compared with those determined from optical microscopy images (not shown). This calibration minimized the potential impact of fluorescent halos on the results. The settings included a scale of 90.91 pixels/mm (2310 dpi), a hue range of 0–255, a saturation range of 36–255, and a brightness range of 165–255. To further analyze MF morphology, fiber lengths were measured in ImageJ by automatically defining regions of interest (ROIs) for each fiber, validated also via manual direct counting to ensure the validity and the robustness of the method. For these analyses, ten filter images were analyzed, totaling thirty samples for both synthetic and washing machine wastewater. Notably, the approach proposed in this study avoids image stitching and extensive sampling, reducing complexity and offering a more accessible, cost-effective alternative to traditional optical microscopy.

2.3. Comparison with TOC measurements

To further corroborate the results of MF quantification through the fluorescence-based method, solid-phase total organic carbon (TOC)

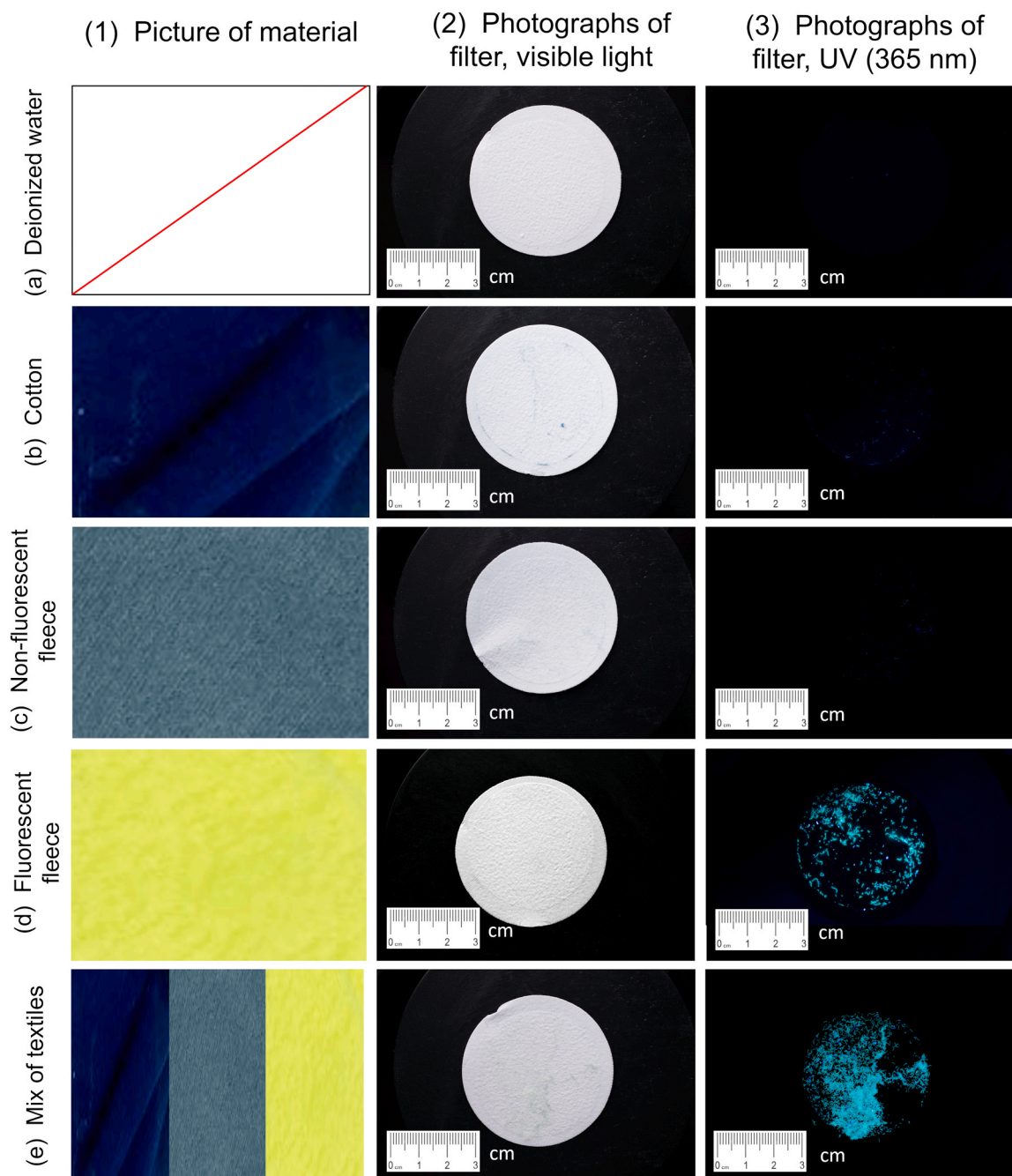


Fig. 4. Images of filter surfaces upon filtration of suspensions containing different textile materials. Rows, from the top: blank sample with only deionized water (a), cotton sample (b), non-fluorescent fleece sample (c), fluorescent fleece sample (d), mixed matrix of fluorescent and non-fluorescent fleece and cotton (e). Columns, from the left: image of the textiles under visible light (1), image of the filter surface under visible light upon filtration of the respective suspension (2), image of the same filter under UV light (3). The scale bars are in cm.

analysis was performed on selected glass fiber filters used for MF suspension filtration. Polyester, comprising approximately 60 % organic carbon by weight, was used as reference material for TOC estimations. A TOC-LCSH/CPH was used, equipped with an SSM-5000A solid sample module (Shimadzu, Japan) featuring a furnace capable of reaching temperatures up to 900 °C, designed to accommodate single solid samples within dedicated ceramic vessels. The sample was prepared by carefully folding the glass fibers filter into eight sections, ensuring the fibers were securely enclosed within the filter to minimize potential microfiber loss during analysis. The carbon content of the sample was determined and subsequently corrected by subtracting the average carbon value obtained from blank filters. These blanks were prepared by

filtering either 1 L of deionized water or washing machine blank water, depending on whether synthetic or washing machine wastewater samples were analyzed. Finally, the measured polyester content was converted into a concentration in mg/L, using the known carbon percentage in polyester and the volume of the filtered sample. The same procedure was adopted for the samples obtained from the washing machine. To accurately determine the average amount of MFs released in each washing cycle, the entirety of the laundry wastewater (roughly 50 L) was filtered through a glass fiber filter. The weight of the filters was directly measured using the analytical balance after drying, and the amount of MFs present in the laundry wastewater was determined as the difference in weight. An average amount of MFs of 3.2 mg/L was thus

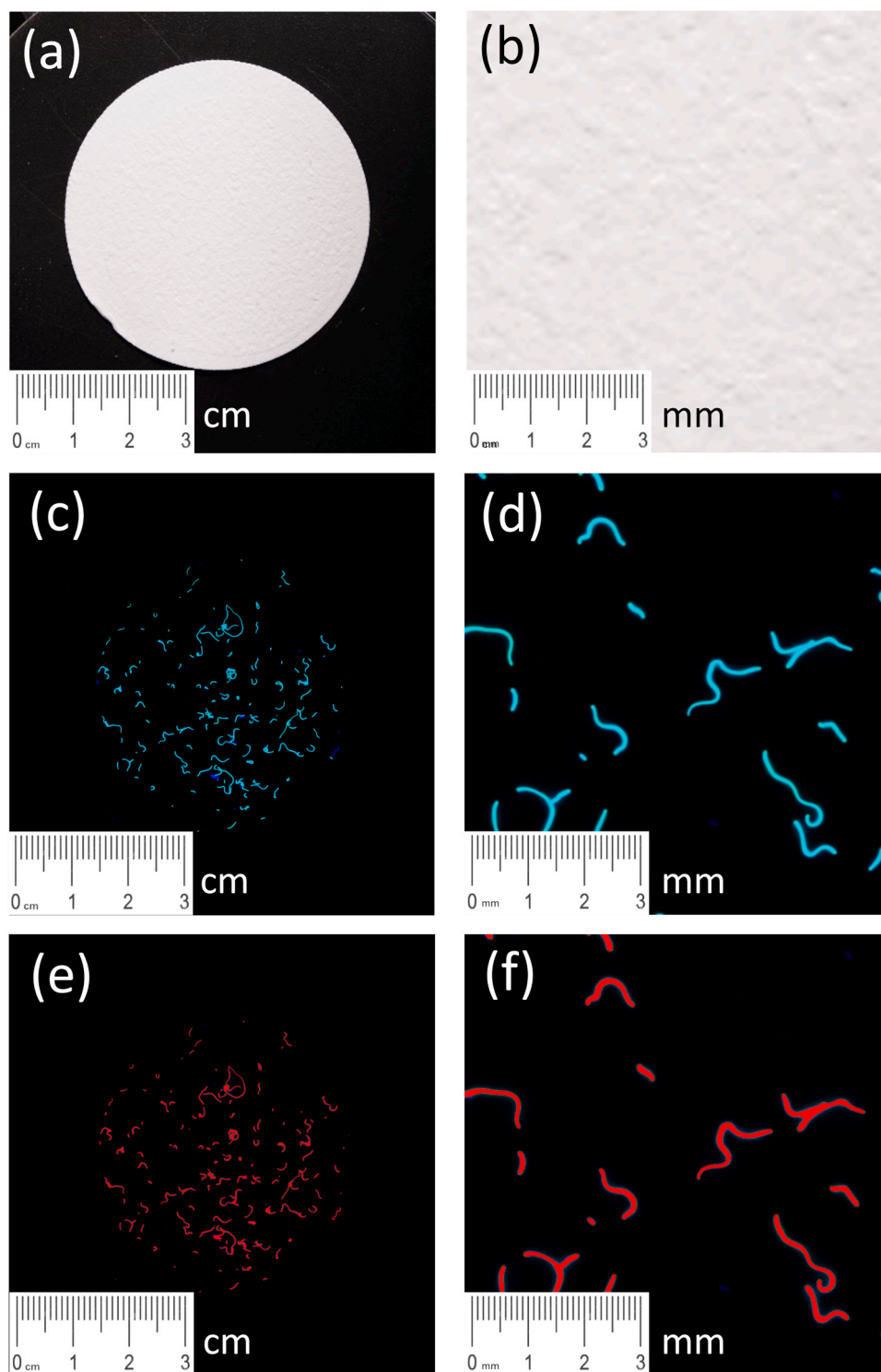


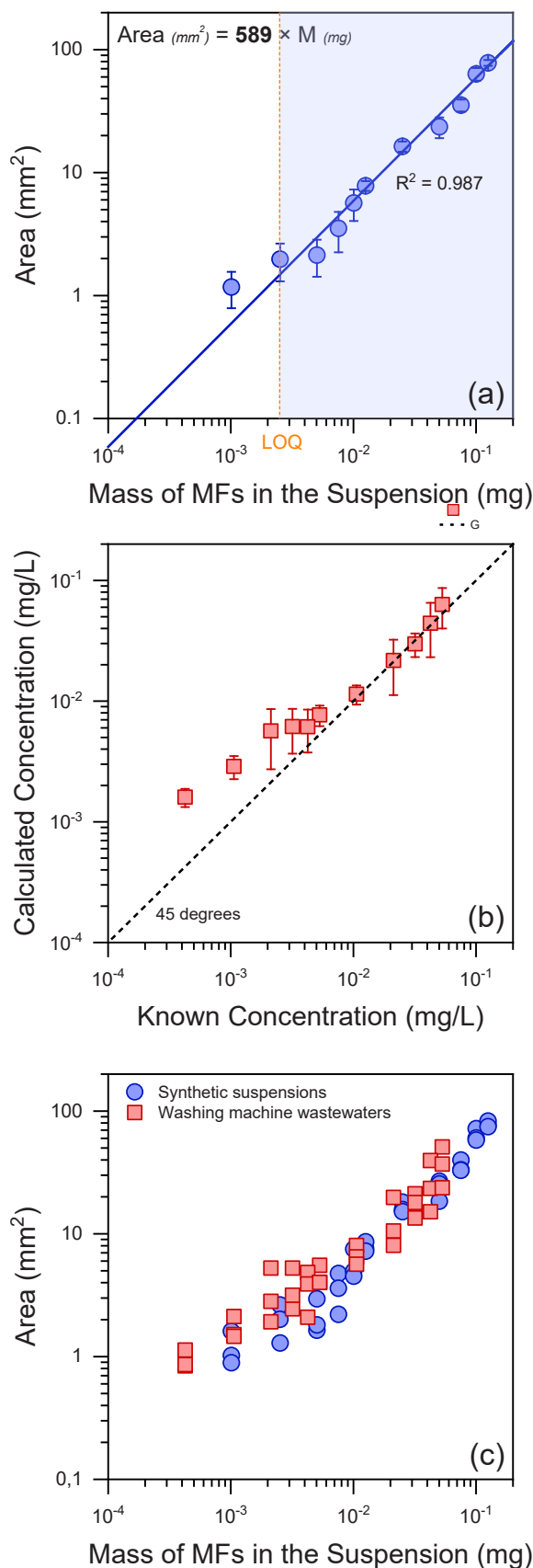
Fig. 5. Representative images of filter surfaces after filtration of a microfiber suspension with a nominal concentration of 0.05 mg/L (1 L of suspension passed through the filter). Left-hand panels report images obtained under visible light (a), under UV light (c), following software processing of the image (e): the scale bars are in cm. Right-hand panels (b), (d), and (f) report a magnified portion of the respective left-hand images: here, the scale bars are in mm.

determined (related to an average concentration of roughly 0.064 mg/L in laundering wastewater).

3. Results and discussion

3.1. Filters and materials characterization and compatibility

The front face excitation-emission matrices (FF-EEM) of the textile, presented in Fig. 3, confirmed a distinct emission peak in the green range (between 480 and 520 nm) for the fluorescent fleece, with the



(caption on next column)

Fig. 6. Development and validation of the fluorescence-based method. (a) Computed microfiber area on filter surfaces versus known MF mass in the suspension: the blue circles represent the average value and standard deviation of replicate measurements, the line indicates a linear fitting with fixed intercept at $y = 0$, with value of R^2 reported for the calibration line. The shaded region represents the area above the limit of quantification (LOQ). (b) Comparison of calculated versus known concentrations for washing machine wastewater samples, showing alignment with the 45-degree line, the latter indicating perfect match between calculated and known concentrations. The red squares represent the average value and standard deviation of replicate analyses. (c) Area values for synthetic (blue circles) and wash water (red squares) samples, plotted across mass ranges. In all cases, 1 L of MF suspension was processed through the filter prior to imaging. Note that all graphs use a log-log scale.

sample displaying an excitation response below 520 nm. This ensures effective spectral separation between an incident ultraviolet light and the minimum emitted wavelength of 480 nm.

Fig. 4 illustrates the results and supports the method's selectivity. The blank sample (Fig. 4a, first row) confirms both the filter's transparency at 365 nm excitation and the purity of water with no MFs visible under either visible or UV light. In Fig. 4b and Fig. 4c (second and third rows), fibers from cotton and non-fluorescent fleece, respectively, are visible under visible light but are absent under UV light. In contrast, Fig. 4d, which refers to a fluorescent fleece sample, shows fibers under visible light but distinctly highlights only fluorescent MFs under the UV source. The same results were obtained from a mixed matrix of cotton, non-fluorescent fleece, and fluorescent fleece (Fig. 4e). See Figure S3 in SI for images at higher magnification.

3.2. Standardization and validation of the fluorescent-based method

Fig. 5 displays representative images of filter surfaces for an MF suspension containing a nominal MF mass equal to 0.05 mg, captured under UV and visible light. The UV image exhibits substantially enhanced contrast, owing to the fluorescence properties of polyester fibers. The MFs appear bright and well-defined against the dark background, allowing straightforward visualization and quantification. In contrast, the visible light image lacks this distinction, with MFs blending into the background. This distinct visualization enables precise counting of the fibers using the automated procedure. An additional advantage of the method is its ability to exclude potential non-fluorescent contamination. For instance, some carbonate precipitates present as contaminants were sometimes visible under visible light but disappeared completely under UV light. This ensured that the microfiber (MF) counting process remained accurate and unaffected by extraneous substances. The image at the bottom in Fig. 5 illustrates the processed version used for MF area estimation, with the software highlighting identified MFs in red.

The fluorescence-based method exhibited strong linearity and repeatability in quantifying MFs within the range between 1 and 125 μg , as shown in Fig. 6a. The results of the quantification of the area were reliable only for 1-L suspensions with concentrations below 125 $\mu\text{g/L}$, *i. e.*, total MF mass equal to 125 μg . At higher concentrations, MFs tended to overlap excessively, leading to underestimated and unreliable measures. Therefore, the analysis was limited to a nominal concentration range between 1 and 125 $\mu\text{g/L}$, corresponding to a mass of MFs between 1 and 125 μg in the 1-L suspensions. The resulting calibration curve, represented by the equation $\text{Area}(\text{mm}^2) = 589 \times M(\text{mg})$, with M referring to MF mass, had an R^2 value of 0.987, indicating excellent fit and reliability. The limit of detection (LOD) was determined to be as low as 1 μg , while the limit of quantification (LOQ) was approximately 2.5 μg . To exemplify, these values imply that the method would allow reliable quantification of the MF concentration in samples of volume as small as 1 mL as long as their MF concentration is larger than 2.5 mg/L (2.5 mg/L \times 0.001 L = 2.5 μg). Indeed, the larger the available sample volume the lower the quantifiable concentration: in a 10 L sample, an MF

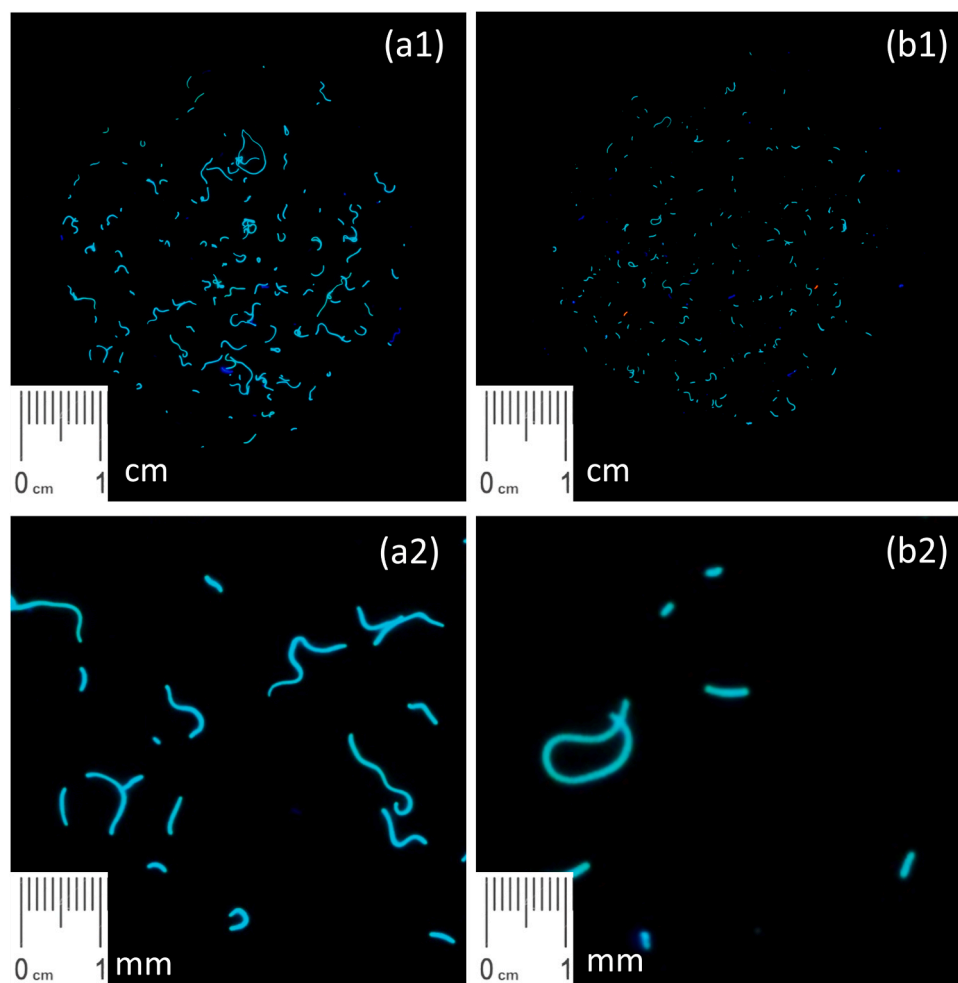


Fig. 7. Representative images taken under UV light of filter surfaces for a synthetic suspension (a1 and a2, left) and a washing machine wastewater sample (b1 and b2, right), both characterized by a nominal microfiber concentration of 0.05 mg/L, with 1 L of each suspension processed through the filter. The scale bars are in cm.

concentration equal to 0.25 $\mu\text{g/L}$ would be sufficient to reach the LOQ (0.25 $\mu\text{g/L} \times 10 \text{ L} = 2.5 \mu\text{g}$). These examples suggest that the method is capable of covering typical concentration ranges in both synthetic and environmental samples and indicate robust performance even at trace concentrations [14]. While this method is particularly valuable for analyses at low concentrations, it is also suitable for analyzing samples with higher concentrations than the practical limit observed in this study (125 μg), provided that rigorous dilutions are performed with special attention to the homogenization phase. The consistency of replicate measurements, evident in the small standard deviations, further highlights the method's precision.

The validation of the method using washing machine wastewater samples (Fig. 6b) demonstrated high accuracy, with computed concentrations using the calibrated equation closely aligning with known values. The deviation from the 45-degree line was minimal, reflecting reliable quantification even for more complex samples. The calibration curve remained effective for washing machine wastewater samples down to masses of approximately 2.5–5 μg , below which minor deviations were observed. Fig. 6c compares the computed area values for synthetic suspensions and washing machine wastewater samples across the tested mass range. While the synthetic samples exhibited consistent linearity, wash water samples displayed a slightly greater variability at lower concentrations. This difference may be attributed to the increased complexity and heterogeneity of washing machine wastewater samples, which can affect the uniform distribution of fibers on the filter. Despite this variability, the overall trend aligned with the calibration curve,

further validating the method's applicability to diverse conditions. Additionally, this result corroborates the method's independence from dilution.

3.3. Morphological insights from synthetic and washing machine wastewater samples

Morphological differences between synthetic and wash water samples are evident in the UV images shown in Fig. 7. Synthetic fibers appeared uniform, with consistent lengths and a relatively smooth appearance, reflecting their controlled preparation. In contrast, wash water samples exhibited greater heterogeneity, with fibers appearing fragmented and polydisperse in size. These differences are attributed to the mechanical, thermal, and chemical degradation experienced by fibers during washing cycles. The visual evidence highlights the potential of this method also to differentiate between controlled and environmentally impacted fibers, providing critical insights into the processes affecting MFs during their lifecycle.

Detailed length analyses, presented in Fig. 8, reveal significant differences in the fiber length distributions of synthetic and wash water samples. Synthetic suspensions exhibited a higher mean fiber length of 2.31 mm, with a narrower and more symmetric distribution. In contrast, washing machine wastewater samples showed a lower mean length of 1.13 mm, with a broader and skewed distribution. The prevalence of shorter fibers (<0.5 mm) in wash water samples once again highlights the extent of fragmentation caused by washing cycles. Box plots in

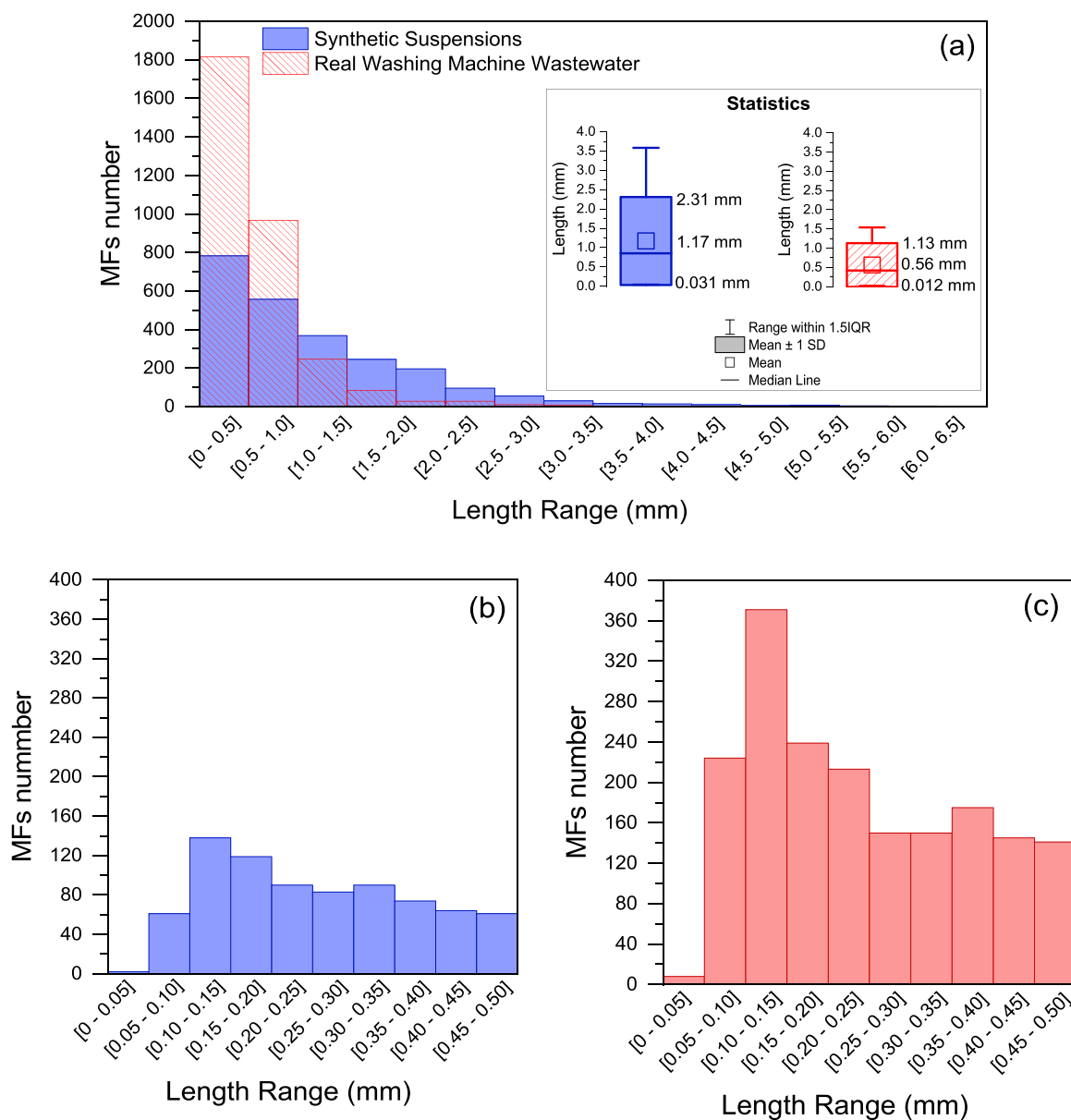


Fig. 8. Microfiber length distribution and statistics. (a, first row) Length distribution over the entire microfiber length range for synthetic suspensions (blue bars) and wastewater (red, patterned bars). The statistics box reports the mean (open square), median (horizontal line within the box), one standard deviation (box height), and the range within the third and the first quartiles with addition and subtraction, respectively, of the interquartile range (IQR) multiplied by 1.5. (b, c, second row) Detailed view of short fibers (<0.5 mm) for synthetic suspensions (b) and wastewater (c).

Fig. 9a also report the statistical summaries of fiber lengths, including means, medians, and interquartile ranges. It is worth noting that in both cases, the majority of MFs fell within the 0–0.5 mm range. Therefore, additional analysis of the length distribution within this range was assessed with results shown in the close-up views of Figs. 9b and 9c. While the data emphasize the dominance of short fibers in wash water samples, the shape of the distributions was found to be similar, particularly within the 0–0.25 mm range, with a peak observed between 0.07 and 0.19 mm. Furthermore, as the amount and length of the fibers increased, a slight increase in the presence of the fluorescent halo was observed following photographic capture. This phenomenon was carefully considered during the image processing phase, serving as a critical factor in calibrating the image parameters.

Figs. 9a and 9b provide additional insights by examining the relationship between total fiber length, computed area, and fiber number. The total length, shown in Fig. 9a, correlates strongly with the computed area for both synthetic and wash water samples, reflecting the uniform

diameter of fibers across all conditions. Despite the overlap in total length, Fig. 9b reveals significant differences in the total number of fibers. Washing machine wastewater samples consistently showed higher fiber counts than synthetic samples for equivalent computed areas. This discrepancy further supports the fragmentation of the fibers in samples during washing discussed above, leading to a greater number of shorter fibers. The observed differences in fiber numbers suggest that laundering processes alter fiber morphology in ways that could influence their environmental fate, transport, and interactions with biota. These findings reinforce the method's capability to capture both quantitative and morphological aspects of MF pollution, making it a valuable tool for comprehensive environmental assessments.

4. Limitations and possible future developments

Although the current methodology performs well under controlled conditions, there are opportunities for further development to broaden

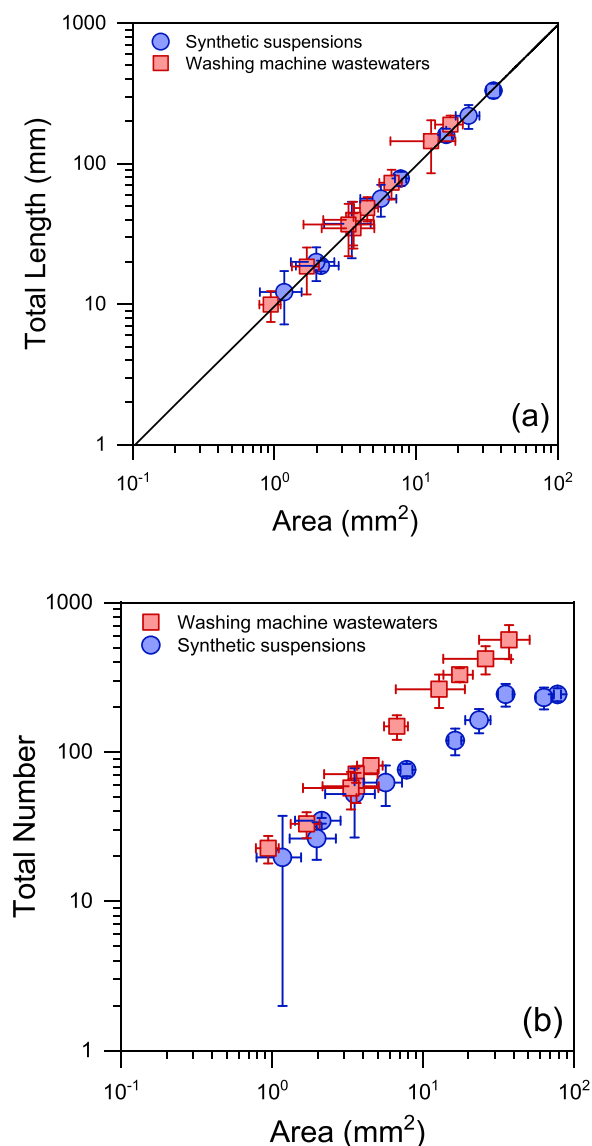


Fig. 9. Quantification of (a) total length and (b) total numbers of the microfibers computed on the filter surfaces as a function of the computed area. In (a), total length refers to the sum of the length of all the individual fibers detected on the filter for each sample. The data points (blue circles for synthetic samples and red squares for washing machine wastewater) represent the average and one standard deviation (for both the y and the x values) for each nominal mass. Note that the graphs use a log-log scale.

its applicability. At present, it is optimized for the detection of synthetic polyester with intrinsic fluorescence and may have limited capacity to distinguish between materials exhibiting similar excitation-emission characteristics. Nonetheless, differentiation could be achievable for materials with sufficiently distinct emission profiles, either under the same, alternative or multiple excitation sources. Moreover, the method could be extended through the use of fluorescent dyes emitting at different wavelengths, allowing for the selective labeling and identification of various polymer types—including both synthetic and natural fibers. Future research should aim to validate and refine the technique for such applications and assess its robustness in more complex matrices containing mixed fibers and potential interferences such as organic matter, surfactants, metals, or precipitates.

5. Conclusions

The fluorescence-based method standardized and validated in this study proved effective for the precise quantification of MF in both synthetic and washing machine wastewater samples. The UV images highlighted the method's ability to clearly distinguish fluorescent, polyester fibers, allowing accurate quantification for MF masses ranging from 2.5 to 125 μg . For concentrated samples, application of the method would require filtration of small water volumes, possibly preceded by careful dilution, with the goal to reach a filtered mass below this maximum level. Analogously, very diluted samples would require filtration of large volumes to fall within the mass range within which quantification was shown to be reliable. By leveraging the fluorescence properties of polyester fibers, the approach enabled direct visualization and quantification with minimal sample preparation, addressing key limitations such as high costs and labor-intensive workflows associated with conventional methods.

Validation with washing machine wastewater samples demonstrated high accuracy, with measured concentrations closely matching known values. Morphological analyses revealed significant differences between synthetic and wash water fibers (1.13 mm vs. 2.31 mm for synthetic samples), showcasing the method's ability to also differentiate between controlled and environmentally impacted fibers. The fiber length distribution showed greater fragmentation in wash water samples, suggesting that washing processes alter the morphology of the fibers, in turn affecting their environmental behavior. The fluorescence-based method's simplicity, affordability, and versatility make it accessible for diverse applications, including academic research, industrial monitoring, and environmental assessments. Its adaptability also makes it suitable for implementation in resource-limited settings, where access to advanced analytical tools is constrained.

Environmental Implication

This study standardizes a fluorescence-based detection method to enhance the accuracy and accessibility of microfiber (MF) quantification, addressing a critical gap in environmental monitoring. The findings reveal extensive fiber fragmentation during laundering, increasing their dispersal and potential environmental impact. By providing a cost-effective tool for monitoring fluorescent MF pollution, this method supports mitigation strategies to reduce their release and environmental footprint. Its simplicity and scalability may aid regulatory efforts and advance sustainable textile management to minimize microfiber pollution in freshwater and marine ecosystems, where their long-term accumulation poses risks to biodiversity and water quality.

CRediT authorship contribution statement

Rajandrea Sethi: Writing – original draft, Validation, Supervision, Resources, Project administration, Methodology, Funding acquisition, Conceptualization. **Alberto Tiraferri:** Writing – review & editing, Writing – original draft, Visualization, Validation, Supervision, Formal analysis, Data curation. **Monica Granetto:** Methodology, Investigation. **Silvia Lupato:** Writing – original draft, Visualization, Software, Investigation.

Declaration of Competing Interest

The authors declare that they have no known competing financial interests or personal relationships that could have appeared to influence the work reported in this paper.

Acknowledgment

This study was carried out within the RETURN (Multi-Risk sciEnce for resilient commUNITies under a changiNg climate) Extended

Partnership and received funding from the European Union NextGenerationEU (Piano Nazionale di Ripresa e Resilienza PNRR, Grant agreement no. PE00000005). The experimental activity was performed in the interdepartmental Clean Water Center (CWC). We would like to thank Haier for providing the washing machine and dryer, and Dr. Martinello for the valuable discussions and insightful suggestions.

Appendix A. Supporting information

Supplementary data associated with this article can be found in the online version at [doi:10.1016/j.jhazmat.2025.138947](https://doi.org/10.1016/j.jhazmat.2025.138947).

Data availability

Data will be made available on request.

References

- Thompson, R.C., Moore, C.J., vom Saal, F.S., Swan, S.H., 2009. Plastics, the environment and human health: current consensus and future trends. *Philos Trans R Soc B Biol Sci* 364 (1526), 2153–2166. <https://doi.org/10.1098/rstb.2009.0053>.
- Carnevale Miino, M., Galafassi, S., Zullo, R., Torretta, V., Rada, E.C., 2024. Microplastics removal in wastewater treatment plants: A review of the different approaches to limit their release in the environment. *Sci Total Environ* 930, 172675. <https://doi.org/10.1016/j.scitotenv.2024.172675>.
- Pagliaccia, B., Ascolese, M., Vannini, E., Carretti, E., Lubello, C., Gori, R., 2025. Methodologic insights aimed to set-up an innovative Laser Direct InfraRed (LDIR)-based method for the detection and characterization of microplastics in wastewaters. *Sci Total Environ* 967, 178817. <https://doi.org/10.1016/j.scitotenv.2025.178817>.
- Fiore, L., Serranti, S., Mazziotti, C., Riccardi, E., Benzi, M., Bonifazi, G., 2022. Classification and distribution of freshwater microplastics along the Italian Po river by hyperspectral imaging. *Environ Sci Pollut Res* 29 (32), 48588–48606. <https://doi.org/10.1007/s11356-022-18501-x>.
- Kye, H., Kim, J., Ju, S., Lee, J., Lim, C., Yoon, Y., 2023. Microplastics in water systems: a review of their impacts on the environment and their potential hazards. *Heliyon* 9 (3). <https://doi.org/10.1016/j.heliyon.2023.e14359>.
- Stapleton, M.J., Hai, F.I., 2023. Microplastics as an emerging contaminant of concern to our environment: a brief overview of the sources and implications. *Bioengineered* 14 (1), 2244754. <https://doi.org/10.1080/21655979.2023.2244754>.
- González-Pleiter, M., Tamayo-Belda, M., Pulido-Reyes, G., Amarie, G., Leganés, F., Rosal, R., Fernández-Piñas, F., 2019. Secondary nanoplastics released from a biodegradable microplastic severely impact freshwater environments. *Environmental Science Nano* 6 (5), 1382–1392. <https://doi.org/10.1039/C8EN01427B>.
- Zhang, K., Hamidian, A.H., Tubić, A., Zhang, Y., Fang, J.K.H., Wu, C., Lam, P.K.S., 2021. Understanding plastic degradation and microplastic formation in the environment: a review. *Environ Pollut* 274, 116554. <https://doi.org/10.1016/j.envpol.2021.116554>.
- Lamichhane, G., Acharya, A., Marahatha, R., Modi, B., Paudel, R., Adhikari, A., Raut, B.K., Aryal, S., Parajuli, N., 2023. Microplastics in environment: global concern, challenges, and controlling measures. *Int J Environ Sci Technol* 20 (4), 4673–4694. <https://doi.org/10.1007/s13762-022-04261-1>.
- da Costa, J.P., Duarte, A.C., Rocha-Santos, T.A.P., 2017. Chapter 1 - Microplastics – Occurrence, Fate and Behaviour in the Environment. In: Rocha-Santos, T.A.P., Duarte, A.C. (Eds.), *Comprehensive Analytical Chemistry*. Elsevier, pp. 1–24. <https://doi.org/10.1016/bs.coac.2016.10.004>.
- Rossi, M., Vergara, A., Capozzi, F., Giordano, S., Spagnuolo, V., Troisi, R., Vedi, V., Ambrosi de Magistris, F., Fiaschini, N., Tommasi, T., Guida, M., D'Aniello, M., Donadio, C., 2024. A new green protocol for the identification of microplastics and microfibers in marine sediments, a case study from the Vesuvian Coast, Southern Italy. *J Hazard Mater* 477, 135272. <https://doi.org/10.1016/j.jhazmat.2024.135272>.
- Gaylarde, C., Baptista-Neto, J.A., da Fonseca, E.M., 2021. Plastic microfibre pollution: how important is clothes' laundering? *Heliyon* 7 (5). <https://doi.org/10.1016/j.heliyon.2021.e07105>.
- Liu, J., Yang, Y., Ding, J., Zhu, B., Gao, W., 2019. Microfibers: a preliminary discussion on their definition and sources. *Environ Sci Pollut Res* 26 (28), 29497–29501. <https://doi.org/10.1007/s11356-019-06265-w>.
- Mishra, S., Singh, R.P., Rath, C.C., Das, A.P., 2020. Synthetic microfibers: Source, transport and their remediation. *J Water Process Eng* 38, 101612. <https://doi.org/10.1016/j.jwpe.2020.101612>.
- Vassilenko, E., Watkins, M., Chastain, S., Mertens, J., Posacka, A.M., Patankar, S., Ross, P.S., 2021. Domestic laundry and microfiber pollution: Exploring fiber shedding from consumer apparel textiles. *PLoS ONE* 16 (7). <https://doi.org/10.1371/journal.pone.0250346>.
- Barcelo, D., Kostianoy, A.G., 2018. *Freshwater Microplastics*. Springer, Cham. <https://doi.org/10.1007/978-3-319-61615-5>.
- Ahmad Wagay, S., Sheikh, J., 2024. Microfibre pollution: An emerging contaminant, alarming threat to the global environment. *J Environ Manag* 371, 123055. <https://doi.org/10.1016/j.jenvman.2024.123055>.
- Barrows, A.P.W., Cathey, S.E., Petersen, C.W., 2018. Marine environment microfiber contamination: Global patterns and the diversity of microparticle origins. *Environ Pollut* 237, 275–284. <https://doi.org/10.1016/j.envpol.2018.02.062>.
- Dos Santos, Nd.O., Busquets, R., Campos, L.C., 2023. Insights into the removal of microplastics and microfibres by Advanced Oxidation Processes. *Sci Total Environ* 861, 160665. <https://doi.org/10.1016/j.scitotenv.2022.160665>.
- Rodríguez-Sejio, A., Pereira, R., 2017. Chapter 3 - Morphological and Physical Characterization of Microplastics. In: Rocha-Santos, T.A.P., Duarte, A.C. (Eds.), *Comprehensive Analytical Chemistry*. Elsevier, pp. 49–66. <https://doi.org/10.1016/bs.coac.2016.10.007>.
- Rosal, R., 2021. Morphological description of microplastic particles for environmental fate studies. *Mar Pollut Bull* 171, 112716. <https://doi.org/10.1016/j.marpolbul.2021.112716>.
- Acharya, S., Rumi, S.S., Hu, Y., Abidi, N., 2021. Microfibers from synthetic textiles as a major source of microplastics in the environment: a review. *Text Res J* 91 (17–18), 2136–2156. <https://doi.org/10.1177/0040517521991244>.
- Hidalgo-Ruz, V., Gutow, L., Thompson, R.C., Thiel, M., 2012. Microplastics in the marine environment: a review of the methods used for identification and quantification. *Environ Sci Technol* 46 (6), 3060–3075. <https://doi.org/10.1021/es203150s>.
- Huppertsberg, S., Knepper, T.P., 2018. Instrumental analysis of microplastics—benefits and challenges. *Anal Bioanal Chem* 410 (25), 6343–6352. <https://doi.org/10.1007/s00216-018-1210-8>.
- Randhawa, J.S., 2023. Advanced analytical techniques for microplastics in the environment: a review. *Bull Natl Res Cent* 47 (1), 174. <https://doi.org/10.1186/s42269-023-01148-0>.
- Rocha-Santos, T., Duarte, A.C., 2015. A critical overview of the analytical approaches to the occurrence, the fate and the behavior of microplastics in the environment. *TrAC Trends Anal Chem* 65, 47–53. <https://doi.org/10.1016/j.trac.2014.10.011>.
- Mishra, S., Dash, D., Das, A.P., 2022. Detection, characterization and possible biofragmentation of synthetic microfibers released from domestic laundering wastewater as an emerging source of marine pollution. *Mar Pollut Bull* 185, 114254. <https://doi.org/10.1016/j.marpolbul.2022.114254>.
- Hale, R.C., Seeley, M.E., La Guardia, M.J., Mai, L., Zeng, E.Y., 2020. A global perspective on microplastics. *J Geophys Res Oceans* 125 (1), e2018JC014719. <https://doi.org/10.1029/2018JC014719>.
- Primpke, S., A. Dias, P., Gerdt, G., 2019. Automated identification and quantification of microfibres and microplastics. *Anal Methods* 11 (16), 2138–2147. <https://doi.org/10.1039/C9AY00126C>.
- Xu, J.-L., Thomas, K.V., Luo, Z., Gowen, A.A., 2019. FTIR and Raman imaging for microplastics analysis: State of the art, challenges and prospects. *TrAC Trends Anal Chem* 119, 115629. <https://doi.org/10.1016/j.trac.2019.115629>.
- Wellner, N., 2013. Fourier transform infrared (FTIR) and Raman microscopy: principles and applications to food microstructures. In: Morris, V.J., Groves, K. (Eds.), *Food Microstructures*, 6. Woodhead Publishing, pp. 163–191. <https://doi.org/10.1533/9780857098894.1.163>.
- Giannattasio, A., Iuliano, V., Oliva, G., Giaquinto, D., Capacchione, C., Cuomo, M. T., Hasan, S.W., Choo, K.-H., Korshin, G.V., Barceló, D., Belgiojorno, V., Grassi, A., Náddeo, V., Buonerba, A., 2024. Micro(nano)plastics from synthetic oligomers persisting in Mediterranean seawater: comprehensive NMR analysis, concerns and origins. *Environ Int* 190, 108839. <https://doi.org/10.1016/j.envint.2024.108839>.
- Dey, T.K., Uddin, M.E., Jamal, M., 2021. Detection and removal of microplastics in wastewater: evolution and impact. *Environ Sci Pollut Res* 28 (14), 16925–16947. <https://doi.org/10.1007/s11356-021-12943-5>.
- Sheikhi, M., Lupato, S., Bianco, C., Sethi, R., Tiraferri, A., 2024. Plastic microfibers from household textile laundering: a critical review of their release and impact reduction. *Crit Rev Environ Sci Technol* 54 (20), 1501–1525. <https://doi.org/10.1080/10643389.2024.2329513>.
- Hong, Y., Oh, J., Lee, I., Fan, C., Pan, S.-Y., Jang, M., Park, Y.-K., Kim, H., 2021. Total-organic-carbon-based quantitative estimation of microplastics in sewage. *Chem Eng J* 423, 130182. <https://doi.org/10.1016/j.cej.2021.130182>.
- Maes, T., Jessop, R., Wellner, N., Haupt, K., Mayes, A.G., 2017. A rapid-screening approach to detect and quantify microplastics based on fluorescent tagging with Nile Red. *Sci Rep* 7 (1), 44501. <https://doi.org/10.1038/srep44501>.
- Prata, J.C., Reis, V., Matos, J.T.V., da Costa, J.P., Duarte, A.C., Rocha-Santos, T., 2019. A new approach for routine quantification of microplastics using Nile Red and automated software (MP-VAT). *Sci Total Environ* 690, 1277–1283. <https://doi.org/10.1016/j.scitotenv.2019.07.060>.
- Shim, W.J., Song, Y.K., Hong, S.H., Jang, M., 2016. Identification and quantification of microplastics using Nile Red staining. *Mar Pollut Bull* 113 (1), 469–476. <https://doi.org/10.1016/j.marpolbul.2016.10.049>.
- Shruti, V.C., Pérez-Guevara, F., Roy, P.D., Kutralam-Muniasamy, G., 2022. Analyzing microplastics with Nile Red: Emerging trends, challenges, and prospects. *J Hazard Mater* 423, 127171. <https://doi.org/10.1016/j.jhazmat.2021.127171>.
- Goldstein, J.I., Newbury, D.E., Michael, J.R., Ritchie, N.W.M., Scott, J.H.J., Joy, D. C., 2018. *Scanning Electron Microscopy and X-Ray Microanalysis*. Springer New York, NY. <https://doi.org/10.1007/978-1-4939-6676-9>.
- Vernon-Parry, K.D., 2000. Scanning electron microscopy: an introduction. *IIIVS Res* 13 (4), 40–44. [https://doi.org/10.1016/S0961-1290\(00\)80006-X](https://doi.org/10.1016/S0961-1290(00)80006-X).
- Zhou, W., Apkarian, R., Wang, Z.L., Joy, D., 2007. Fundamentals of Scanning Electron Microscopy (SEM). In: Zhou, W., Wang, Z.L. (Eds.), *Scanning Microscopy*

- for Nanotechnology: Techniques and Applications. Springer New York, New York, NY, pp. 1–40. https://doi.org/10.1007/978-0-387-39620-0_1.
- [43] Berthomieu, C., Hienerwadel, R., 2009. Fourier transform infrared (FTIR) spectroscopy. *Photosynth Res* 101 (2), 157–170. <https://doi.org/10.1007/s11120-009-9439-x>.
- [44] Ismail, A.A., van de Voort, F.R., Sedman, J., 1997. Chapter 4 Fourier transform infrared spectroscopy: Principles and applications. In: Paré, J.R.J., Bélanger, J.M.R. (Eds.), *Techniques and Instrumentation in Analytical Chemistry*. Elsevier, pp. 93–139. [https://doi.org/10.1016/S0167-9244\(97\)80013-3](https://doi.org/10.1016/S0167-9244(97)80013-3).
- [45] Mulvaney, S.P., Keating, C.D., 2000. Raman Spectroscopy. *Anal Chem* 72 (12), 145–158. <https://doi.org/10.1021/a10000155>.
- [46] Della Ventura, G., Bellatreccia, F., Marcelli, A., Cestelli Guidi, M., Piccinini, M., Cavallo, A., Piochi, M., 2010. Application of micro-FTIR imaging in the Earth sciences. *Anal Bioanal Chem* 397 (6), 2039–2049. <https://doi.org/10.1007/s00216-010-3811-8>.
- [47] Kawata, S., Ichimura, T., Taguchi, A., Kumamoto, Y., 2017. Nano-Raman Scattering Microscopy: Resolution and Enhancement. *Chem Rev* 117 (7), 4983–5001. <https://doi.org/10.1021/acs.chemrev.6b00560>.
- [48] Amirav, A., Keshet, U., Alon, T., Fialkov, A.B., 2014. Open Probe fast GC–MS—Real time analysis with separation. *Int J Mass Spectrom* 371, 47–53. <https://doi.org/10.1016/j.ijms.2014.08.002>.
- [49] Hermabessiere, L., Himber, C., Boricaud, B., Kazour, M., Amara, R., Cassone, A.-L., Laurentie, M., Paul-Pont, I., Soudant, P., Dehaut, A., Duflos, G., 2018. Optimization, performance, and application of a pyrolysis-GC/MS method for the identification of microplastics. *Anal Bioanal Chem* 410 (25), 6663–6676. <https://doi.org/10.1007/s00216-018-1279-0>.
- [50] Li, P., Lai, Y., Li, Q., Dong, L., Tan, Z., Yu, S., Chen, Y., Sharma, V.K., Liu, J., Jiang, G., 2022. Total Organic Carbon as a Quantitative Index of Micro- and Nano-Plastic Pollution. *Anal Chem* 94 (2), 740–747. <https://doi.org/10.1021/acs.analchem.1c03114>.
- [51] Tian, Y., Chen, Z., Zhang, J., Wang, Z., Zhu, Y., Wang, P., Zhang, T., Pu, J., Sun, H., Wang, L., 2021. An innovative evaluation method based on polymer mass detection to evaluate the contribution of microfibers from laundry process to municipal wastewater. *J Hazard Mater* 407, 124861. <https://doi.org/10.1016/j.jhazmat.2020.124861>.
- [52] Lim, S.J., Park, Y.-K., Kim, H., Kwon, J., Moon, H.M., Lee, Y., Watanabe, A., Teramae, N., Ohtani, H., Kim, Y.-M., 2022. Selective solvent extraction and quantification of synthetic microfibers in textile laundry wastewater using pyrolysis-gas chromatography/mass spectrometry. *Chem Eng J* 434, 134653. <https://doi.org/10.1016/j.cej.2022.134653>.
- [53] Galvão, A., Aleixo, M., De Pablo, H., Lopes, C., Raimundo, J., 2020. Microplastics in wastewater: microfiber emissions from common household laundry. *Environ Sci Pollut Res* 27 (21), 26643–26649. <https://doi.org/10.1007/s11356-020-08765-6>.
- [54] Haap, J., Classen, E., Beringer, J., Mecheels, S., Gutmann, J.S., 2019. Microplastic fibers released by textile laundry: a new analytical approach for the determination of fibers in effluents. *Water* 11 (10). <https://doi.org/10.3390/w11102088>.
- [55] Serranti, S., Capobianco, G., Cucuzza, P., Bonifazi, G., 2024. Efficient microplastic identification by hyperspectral imaging: a comparative study of spatial resolutions, spectral ranges and classification models to define an optimal analytical protocol. *Sci Total Environ* 954, 176630. <https://doi.org/10.1016/j.scitotenv.2024.176630>.
- [56] Serranti, S., Palmieri, R., Bonifazi, G., Cózar, A., 2018. Characterization of microplastic litter from oceans by an innovative approach based on hyperspectral imaging. *Waste Manag* 76, 117–125. <https://doi.org/10.1016/j.wasman.2018.03.003>.
- [57] Napper, I.E., Thompson, R.C., 2016. Release of synthetic microplastic plastic fibres from domestic washing machines: Effects of fabric type and washing conditions. *Mar. Pollut. Bull.* 112 (1–2), 39–45. <https://doi.org/10.1016/j.marpolbul.2016.09.025>.
- [58] De Falco, F., Di Pace, E., Cocca, M., Avella, M., Scholz, B., Fox, R., Mayershofer, M., 2020. First Investigation of Microfibre Release from the Washing of Laminated Fabrics for Outdoor Apparel. *Springer Water* 277–281. https://doi.org/10.1007/978-3-030-45909-3_44.
- [59] De Falco, F., Cocca, M., Avella, M., Thompson, R.C., 2020. Microfiber Release to Water, Via Laundering, and to Air, via Everyday Use: A Comparison between Polyester Clothing with Differing Textile Parameters. *Environ. Sci. Technol.* 54 (6), 3288–3296. <https://doi.org/10.1021/acs.est.9b06892>.
- [60] Ye, Y., Yu, K., Zhao, Y., 2022. The development and application of advanced analytical methods in microplastics contamination detection: a critical review. *Sci Total Environ* 818, 151851. <https://doi.org/10.1016/j.scitotenv.2021.151851>.
- [61] Tarte, J.V., Johir, M.A.H., Tra, V.-T., Cai, Z., Wang, Q., Nghiem, L.D., 2024. Optimising microplastics analysis for quantifying and identifying microplastic fibres in laundry wastewater. *Sci Total Environ* 952, 175907. <https://doi.org/10.1016/j.scitotenv.2024.175907>.
- [62] Balestra, V., Trunfio, F., Akyıldız, S.H., Marini, P., Bellopede, R., 2024. Microparticles of anthropogenic origin (microplastics and microfibers) in sandy sediments: a case study from Calabria, Italy. *Environ Monit Assess* 196 (10), 993. <https://doi.org/10.1007/s10661-024-13159-z>.
- [63] Velimirovic, M., Tirez, K., Voorspoels, S., Vanhaecke, F., 2021. Recent developments in mass spectrometry for the characterization of micro- and nanoscale plastic debris in the environment. *Anal Bioanal Chem* 413 (1), 7–15. <https://doi.org/10.1007/s00216-020-02898-w>.
- [64] Lanjun, S., Zhijian, L., Xiongfei, M., Yanchao, Z., Shuhan, H., Le, L., Lin, W., 2025. Rapid identification of marine microplastics by laser-induced fluorescence technique based on PCA combined with SVM and KNN algorithm. *Environ Res* 269, 120947. <https://doi.org/10.1016/j.envres.2025.120947>.
- [65] Meng, X., Chen, S., Li, D., Song, Y., Sun, L., 2024. Identification of marine microplastics based on laser-induced fluorescence and principal component analysis. *J Hazard Mater* 465, 133352. <https://doi.org/10.1016/j.jhazmat.2023.133352>.
- [66] Motalebizadeh, A., Fardindoost, S., Hoorfar, M., 2024. Selective on-site detection and quantification of polystyrene microplastics in water using fluorescence-tagged peptides and electrochemical impedance spectroscopy. *J Hazard Mater* 480, 136004. <https://doi.org/10.1016/j.jhazmat.2024.136004>.
- [67] Pramanik, D.D., Kay, P., Goycoolea, F.M., 2024. A rapid and portable fluorescence spectroscopy staining method for the detection of plastic microfibers in water. *Sci Total Environ* 908, 168144. <https://doi.org/10.1016/j.scitotenv.2023.168144>.
- [68] Belfatmi, R., Lamotte, M., Ait-Lyazidi, S., Fournier de Violet, P., 2005. Detection of PCBs in natural waters by front face fluorometry on solid sorbent on account of their fluorescence quantum yields and interaction with humic substances. *Chemosphere* 61 (6), 761–769. <https://doi.org/10.1016/j.chemosphere.2005.03.092>.